International Journal of Modern Physics B
Vol. 17, Nos. 1 & 2 (2003) 41–47

HYBRID FINITE-DIFFERENCE THERMAL LATTICE BOLTZMANN EQUATION

PIERRE LALLEMAND*

Laboratoire ASCI, Bâtiment 506, Université Paris-Sud (Paris XI Orsay)
91405 Orsay Cedex, France

LI-SHI LUO†

ICASE, MS 132C, NASA Langley Research Center
3 West Reid Street, Building 1152, Hampton, Virginia 23681-2199, USA

Received 9 August 2002

We analyze the acoustic and thermal properties of athermal and thermal lattice Boltzmann equation (LBE) in 2D and show that the numerical instability in the thermal lattice Boltzmann equation (TLBE) is related to the algebraic coupling among different modes of the linearized evolution operator. We propose a hybrid finite-difference (FD) thermal lattice Boltzmann equation (TLBE). The hybrid FD-TLBE scheme is far superior over the existing thermal LBE schemes in terms of numerical stability. We point out that the lattice BGK equation is incompatible with the multiple relaxation time model.

1. Introduction

In spite of its success in solving various challenging problems involving athermal fluids, the lattice Boltzmann equation (LBE) has not been able to handle realistic thermal fluids with satisfaction, even though there has been a continuous pursue in this area for obvious reasons.[1–28] The difficulty encountered in the thermal lattice Boltzmann equation (TLBE) seems to be the numerical instabilities.

The existing thermal lattice Boltzmann models may be classified into three categories. The first and the simplest one is to use two sets of distributions for the flow fields and temperature which is treated as a passive scalar.[2–6] Numerically this is not very efficient because of too many redundant degrees of freedom, even though it can be improved somewhat.[5] The second category of the TLBE models includes various shock capturing schemes to simulate fully compressible Euler[7–9] or Navier-Stokes[10–12] equations. The numerical accuracy of these shock capturing schemes remains mostly unknown. It is not clear what benefit these schemes can

*email address: lalleman@asci.fr
†email address: luo@icase.edu; homepage: www.icase.edu/~luo

offer especially when there are other tested shock capturing schemes based on kinetic theory.[29] We shall not further discuss the LBE models in these two categories.

The thermal LBE models in the third category include the (local) energy conservation law, and are characterized by low Mach number and Boussinesq approximations. There are a few proposals to construct a energy-conserving LBE model:

(1) To increase the number of velocities,[13,14] and to include higher order nonlinear terms (of $\boldsymbol{u}$) in the equilibria,[15] or to use equilibria of non-polynomial type.[16]
(2) To use equilibrium distribution functions depending on varying temperature.[13]
(3) To use an advection with finite-difference techniques, such as Lax-Wendroff scheme, to improve numerical stability.[17,18]
(4) To use two sets of distribution functions for particle number density and energy density which effectively doubles the number of discrete velocities.[19–22]
(5) To use a velocity set of better symmetry[23] or energy-dependent velocities,[25] with interpolations that increase numerical viscosities and anisotropic effects.[32]
(6) To use a hybrid scheme in which the LBE flow simulation is decoupled from the solution of the temperature equation by finite-difference techniques.[26,27]

As previously noticed,[1,14,17,24,28] the main difficulty encountered in the TLBE simulations is the numerical instability. However, the true nature of the numerical instability is not yet well understood to this date.

This paper is a summary of our ongoing effort to present a systematic analysis of the origin of the numerical instability encountered in the TLBE schemes, and to propose a practical remedy to overcome this difficulty.[30–31] Section 2 provides a comparative study of athermal and thermal lattice Boltzmann equations with thirteen velocities on a 2D square lattice (denoted as D2Q13S). We observe that the origin of the TLBE models is the algebraic coupling between the viscous mode and the energy mode of the linearized evolution operator of the system. Section 3 describes the proposed hybrid FD-TLBE scheme. Section 4 concludes the paper.

2. 2D Thermal and Athermal LBE Models with 13 Velocities

In the setting of the generalized lattice Boltzmann equation (GLBE) or the moment method,[1,32–34] the lattice Boltzmann equation can be written as

$$|f(\boldsymbol{r}_j + \boldsymbol{c}_i,\, t_n + 1)\rangle = |f(\boldsymbol{r}_j, t_n)\rangle - \mathsf{M}^{-1}\mathsf{S}\left[|m(\boldsymbol{r}_j, t_n)\rangle - |m^{(\mathrm{eq})}(\boldsymbol{r}_j, t_n)\rangle\right], \qquad (1)$$

where $\{\boldsymbol{r}_j\}$ is on a D-dimensional lattice space, $\{\boldsymbol{c}_i | i = 0,\, 1,\, \ldots,\, b\}$ is the discrete velocity set, S is the diagonal matrix of the relaxation rates $\{s_i | i = 1,\, 2,\, \ldots,\, (b{+}1)\}$,

$$\mathsf{S} = \mathrm{diag}(s_1,\, s_2,\, \ldots,\, s_{b+1}),$$

and $|m^{(\mathrm{eq})}\rangle$ is the equilibrium-moment vector the components of which are the equilibria of the moments.[1,32–34]

The equilibria of the non-conserved moments, up to second order in $\boldsymbol{j}$, are:[32]

$$m_4^{(\mathrm{eq})} = e^{(\mathrm{eq})} = \alpha_2 \rho + \beta_2 \boldsymbol{j}\cdot\boldsymbol{j}, \qquad (2)$$

$$m_5^{(\mathrm{eq})} = p_{xx}^{(\mathrm{eq})} = j_x^2 - j_y^2, \qquad m_6^{(\mathrm{eq})} = p_{xy}^{(\mathrm{eq})} = j_x j_y, \tag{3}$$

$$m_7^{(\mathrm{eq})} = \varepsilon^{(\mathrm{eq})} = \alpha_3 \rho, \qquad m_8^{(\mathrm{eq})} = h^{(\mathrm{eq})} = \alpha_4 \rho, \tag{4}$$

$$m_9^{(\mathrm{eq})} = \pi_{xx}^{(\mathrm{eq})} = 0, \tag{5}$$

$$m_{10,12}^{(\mathrm{eq})} = q_{x,y}^{(\mathrm{eq})} = c_1 j_{x,y}, \qquad m_{11,13}^{(\mathrm{eq})} = \eta_{x,y}^{(\mathrm{eq})} = c_2 j_{x,y}. \tag{6}$$

The above equilibria are for the athermal model. As for the (energy conserving) thermal model, the energy e is a conserved quantity, thus its equilibrium is itself, and its relaxation rate s_e is zero. The transformation matrix M for the model is

$$\begin{pmatrix} \langle \rho | \\ \langle j_x | \\ \langle j_y | \\ \langle e | \\ \langle p_{xx} | \\ \langle p_{xy} | \\ \langle \varepsilon | \\ \langle h | \\ \langle \pi_{xx} | \\ \langle q_x | \\ \langle \eta_x | \\ \langle q_y | \\ \langle \eta_y | \end{pmatrix} = \begin{pmatrix} 1 & 1 & 1 & 1 & 1 & 1 & 1 & 1 & 1 & 1 & 1 & 1 & 1 \\ 0 & 1 & 0 & -1 & 0 & 1 & -1 & -1 & 1 & 2 & 0 & -2 & 0 \\ 0 & 0 & 1 & 0 & -1 & 1 & 1 & -1 & -1 & 0 & 2 & 0 & -2 \\ -28 & -15 & -15 & -15 & -15 & -2 & -2 & -2 & -2 & 24 & 24 & 24 & 24 \\ 0 & 1 & -1 & 1 & -1 & 0 & 0 & 0 & 0 & 4 & -4 & 4 & -4 \\ 0 & 0 & 0 & 0 & 0 & 1 & -1 & 1 & -1 & 0 & 0 & 0 & 0 \\ 140 & -2 & -2 & -2 & -2 & -67 & -67 & -67 & -67 & 34 & 34 & 34 & 34 \\ -12 & 8 & 8 & 8 & 8 & -6 & -6 & -6 & -6 & 1 & 1 & 1 & 1 \\ 0 & -4 & 4 & -4 & 4 & 0 & 0 & 0 & 1 & -1 & 1 & -1 & 0 \\ 0 & -2 & 0 & 2 & 0 & -1 & 1 & 1 & -1 & 2 & 0 & -2 & 0 \\ 0 & 4 & 0 & -4 & 0 & -3 & 3 & 3 & -3 & 1 & 0 & -1 & 0 \\ 0 & 0 & -2 & 0 & 2 & -1 & -1 & 1 & 1 & 0 & 2 & 0 & -2 \\ 0 & 0 & -4 & 0 & 4 & 3 & 3 & -3 & -3 & 0 & -1 & 0 & 1 \end{pmatrix}. \tag{7}$$

The evolution equation (1) can be linearized around the state with a constant velocity $\boldsymbol{V}$ to obtain a linearized equation for the fluctuations δf in Fourier space:[32]

$$|\delta f(\boldsymbol{k}, t+1)\rangle = \mathsf{L} |\delta f(\boldsymbol{k}, t)\rangle, \qquad \mathsf{L} = \mathsf{A}^{-1}[\mathsf{I} + \mathsf{M}^{-1}\mathsf{C}\mathsf{M}], \tag{8}$$

where I is the identity matrix, C is the linearized collision operator, and A is the propagation operator which is a diagonal matrix in the space of $|f\rangle$:

$$\mathsf{A} = \mathrm{diag}\left(e^{-i\boldsymbol{k}\cdot\boldsymbol{c}_0},\, e^{-i\boldsymbol{k}\cdot\boldsymbol{c}_1},\, \ldots,\, e^{-i\boldsymbol{k}\cdot\boldsymbol{c}_b}\right).$$

The solution of the eigen-value problem of the linearized evolution operator,

$$\mathsf{L}|\varphi\rangle = z|\varphi\rangle, \tag{9}$$

yields the generalized hydrodynamics of the model, i.e., the $\boldsymbol{k}$-dependence of the transport coefficients, the sound speed, and the Galilean-invariance factor g.[32,35]

We compute attenuation rates for the modes of the linearized operator L for both thermal and athermal D2Q13S models. The results are shown in Fig. 1. We choose a direction with the polar angle $\theta = 22.5° = \pi/8$. For the thermal model, the energy mode (γ_h) and the shear mode ($\gamma_\perp$) coalesce at $k_c \approx 0.047$. Also, the coalescence occurs in a wide range $[k_c, \pi - k_c]$ of the wave-number k along certain directions, hence the energy-conserving TLBE models are prone to numerical instabilities which can be instigated by fluctuations of wide-ranged scales. In contrast, for the athermal LBE models a similar coalescence occurs only when k is near π, making the the athermal LBE models only sensitive to the small scale fluctuations.[32] We also observe that the algebraic coupling between the two modes cannot be removed by increasing the number of discrete velocities.[30] This problem is intrinsic to the linearity of the lattice Boltzmann models.

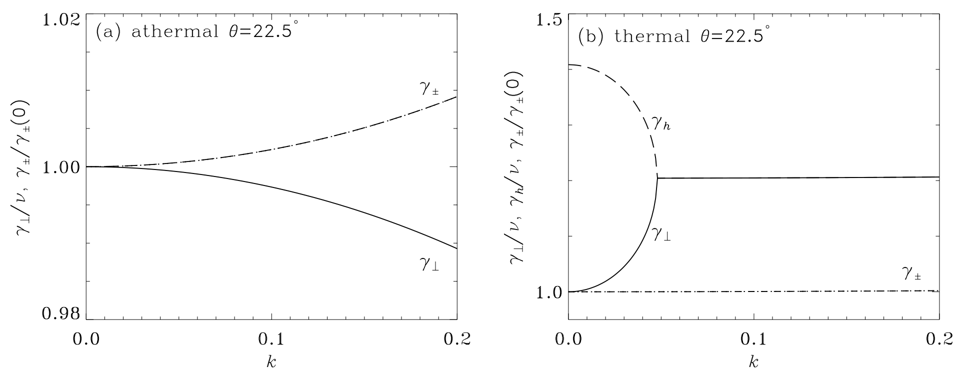

Fig. 1. Attenuation rates of the acoustic modes $\gamma_\pm$, shear mode $\gamma_\perp$, and energy mode γ_h for the athermal and thermal D2Q13S models, along the direction of $\theta = 22.5° = \pi/8$. Parameters used are: $\nu = 0.1$, $s_7 = 1.62$, $s_8 = 1.24$, $s_9 = 1.11$, $s_{10} = 1.938$, and $s_{11} = 1.65$. (a) Athermal D2Q13 model, $s_4 = 1.6$, $c_s^2 = 1/2$. (b) Thermal D2Q13 model, $\gamma = 1.2$, $\mathrm{Pr} = 0.71$, $c_s^2 = 1.2923$.

3. Hybrid TLBE Scheme

To remove the spurious algebraic coupling among the modes, we propose a hybrid lattice Boltzmann equation in which the flow fields are solved by the athermal lattice Boltzmann equation defined by Eq. (1), while the advection-diffusion equation for temperature is solved separately by finite difference technique:

$$T(\boldsymbol{r}_j, t+1) - T(\boldsymbol{r}_j, t) = -\boldsymbol{j}\cdot\boldsymbol{\nabla}_h T + \kappa\Delta_h T + q_2(\gamma - 1)c_{s0}^2\,\boldsymbol{\nabla}_h\cdot\boldsymbol{j}, \tag{10}$$

where $\boldsymbol{\nabla}_h$ and Δ_h stand for finite-difference gradient and Laplacian operators, respectively. It should be stressed that the stencils used in this hybrid scheme must be the ones with the same symmetry of the discrete velocity set.[30] The coupling of temperature to the fluid momentum is explicit in the above equation for T. The coupling of the momentum $\boldsymbol{j}$ to temperature T is in the equilibria of e and ε:

$$e^{(\mathrm{eq})} = \alpha_2\rho + \beta_2\boldsymbol{j}\cdot\boldsymbol{j} + q_1 T, \qquad \varepsilon^{(\mathrm{eq})} = \alpha_3\rho, \tag{11}$$

where both $\alpha_2 = \alpha_2(c_{s0}^2)$ and $\beta_2 = \beta_2(\gamma)$ are determined by the first-order solution of the linearized dispersion equation. And the value of the parameter α_3 is determined so that in the equation for T the term linear in the density gradient $\boldsymbol{\nabla}\rho$ vanishes. The other two coefficients in the model, q_1 and q_2, are determined by the linear analysis so that the hydrodynamic equations derived from the model are

$$\partial_t \rho + \boldsymbol{\nabla}\cdot\boldsymbol{j} = 0, \tag{12}$$

$$\partial_t \boldsymbol{j} + \boldsymbol{j}\cdot\boldsymbol{\nabla}\boldsymbol{j} = -c_{s0}^2 \boldsymbol{\nabla}\rho + \nu\Delta\boldsymbol{j} + \zeta'\boldsymbol{\nabla}\boldsymbol{\nabla}\cdot\boldsymbol{j} + \boldsymbol{\nabla}T, \tag{13}$$

$$\partial_t T + \gamma\boldsymbol{j}\cdot\boldsymbol{\nabla}T = \kappa\Delta T + (\gamma - 1)c_{s0}^2\,\boldsymbol{\nabla}\cdot\boldsymbol{j}, \tag{14}$$

where $\zeta' = \zeta$ in two dimensions and $\zeta' = \zeta + \nu/3$ in three dimensions, c_{s0}, κ and γ are adjustable parameters in the model. Note that γ plays the role of the ratio of specific heats in a real gas. The viscosities ν and ζ are controlled by the relaxation rates s_{xx} and s_e, respectively,

$$\nu = A_\nu(c_1)\left(\frac{1}{s_{xx}} - \frac{1}{2}\right), \qquad \zeta = A_\zeta(c_1, \gamma c_{s0}^2)\left(\frac{1}{s_e} - \frac{1}{2}\right), \tag{15}$$

and the adiabatic sound speed is

$$c_s^2 = \gamma\, c_{s0}^2. \tag{16}$$

The coefficients $A_\nu(c_1)$ and $A_\zeta(c_1, \gamma c_{s0}^2)$ are model dependent.[30] For example, for both D2Q9S and D3Q13 models, $c_1 = -1$, $A_\nu = 1/2$, and $A_\zeta = 2/3 - \gamma c_{s0}^2$.[30]

It should be noted that the isothermal (athermal) sound speed c_{s0} does not depend on the adjustable parameters in the model:

$$c_{s0}^2 = \frac{dp}{d\rho} = \frac{e_K}{\rho} = \frac{1}{2B}\sum_i \boldsymbol{c}_i \cdot \boldsymbol{c}_i, \tag{17}$$

where B is the total number of the discrete velocities (including the zero velocity), and p and e_K are the pressure and the specific kinetic energy.

4. Conclusions

In this paper we propose to solve the thermohydrodynamic equations by using a hybrid lattice Boltzmann scheme: the usual lattice Boltzmann equation is used to solve the mass and momentum conservation equations, while a finite-difference method is used to solve the diffusion-advection equation for the temperature, with proper couplings between the two systems. We have identified that the main culprit of numerical instabilities in the existing thermal lattice Boltzmann models is the coupling between certain hydrodynamic modes of the linearized LBE evolution operator. The finite-difference hybrid thermal lattice Boltzmann method removes the spurious coupling thus significantly improves the numerical stability.

The present work differs from the existing ones in several aspects. First of all, we advocate the MRT model as opposed to the BGK model which is partially responsible for numerical instabilities.[32] In addition, the Prandtl number is adjustable for the MRT models. It should be emphasized that without the flexibility of the MRT model, it is impossible to construct D3Q13 model. Secondly, we have provided a systematic analysis of the proposed hybrid TLBE model, and a comparative study with the existing thermal LBE models.[30] Finally, the proposed hybrid FD-TLBE model does not use the Boussinesq approximation explicitly and can be readily extended to the situations where the Boussinesq approximation is inadequate (*e.g.*, temperature dependent transport coefficients and considerable density variations).

Several 3D simulations by using the thirteen-velocity model in a cubic lattice (D3Q13)[33] have been carried out successfully: Rayleigh-Bénard convection in (1) a differentially heated cubic cavity,[36] and (2) a differentially heated rotating circular cell.[37] The details of these simulations shall be reported elsewhere.[30,31]

Acknowledgments

LSL is partially funded by the US-AFOSR under Grant No. F49620-01-1-0142 (technical monitor: Dr J. Tishkoff), and likes to acknowledge the support from Lab. ASCI for his visit to the Lab. in April, 2002 during which part of this work was done.

References

1. D. d'Humières, in *RGD: Theory and Simulations*, *Progress in Astronautics and Aeronautics* **159**, ed. B.D. Shizgal and D.P. Weaver (AIAA, Washington DC, 1992), p. 450.
2. F. Massaioli, R. Benzi, and S. Succi, *Europhy. Lett.* **21**, 305 (1993).
3. J.G.M. Eggels and J.A. Sommers, *Int. J. Heat Fluid Flow* **16**, 357 (1995).
4. X. Shan, *Phys. Rev.* **E55**, 2780 (1997).
5. S. Succi, G. Bella, and F. Papetti, *J. Scien. Comput.* **12**, 395 (1997).
6. R.G.M. van der Sman *et al.*, *Int. J. Heat Mass Transfer* **43**, 577 (2000).
7. G. Yan, Y. Chen, and S. Hu, *Phys. Rev.* **E59**, 454 (1999).
8. F.L. Hinton *et al.*, *Phys. Rev.* **E63**, 061212 (2001).
9. W. Shi, W. Shyy, and R. Mei, *Numer. Heat Transfer* **B40**, 1 (2001).
10. J. Huang *et al.*, *Int. J. Mod. Phys.* **C8**, 827–841 (1997).
11. C. Sun, *Phys. Rev.* **E58**, 7283 (1998); *ibid* **E61**, 2645 (2000); *J. Computat. Phys.* **161**, 70 (2000).
12. R.J. Mason, *J. Stat. Phys.* **107**, 385 (2002).
13. F.J. Alexander, S. Chen and J.D. Sterling, *Phys. Rev.* **E47**, R2249 (1993).
14. G. McNamara and B.J. Alder, *Physica* **A194**, 218 (1993)
15. Y. Chen, H. Ohashi, and M. Akiyama, *Phys. Rev.* **E50**, 2776 (1994).
16. A. Renda, G. Bella, S. Succi, and I.V. Karlin, *Europhy. Lett.* **41**, 279 (1998)
17. G. McNamara, A. Garcia and B.J. Alder, *J. Stat. Phys.* **81**, 395 (1995).
18. G. McNamara, A. Garcia and B.J. Alder, *J. Stat. Phys.* **87**, 1111 (1997).
19. X. He, S. Chen and G.D. Doolen, *J. Computat. Phys.* **146**, 282 (1998).
20. B.J. Palmer and D.R. Rector, *J. Computat. Phys.* **161**, 1 (2000).
21. B.J. Palmer and D.R. Rector, *Phys. Rev.* **E61**, 5295 (2000).
22. T. Ihle and D.M. Kroll, *Comput. Phys. Comm.* **129**, 1 (2000).
23. P. Pavlo *et al.*, *J. Computat. Phys.* **139**, 79 (1998); M. Soe *et al.*, *Phys. Rev.* **E57**, 4227 (1998); G. Vahala *et al.*, *Int. J. Mod. Phys.* **C9**, 1247 (1998); L. Vahala *et al.*, *Phys. Rev.* **E62**, 507 (2000).
24. P. Pavlo, G. Vahala, L. Vahala, and M. Soe, *J. Computat. Phys.* **139**, 79 (1998).
25. P. Pavlo, G. Vahala, and L. Vahala, *J. Stat. Phys.* **107**, 499 (2002).
26. O. Filippova and D. Hänel, *Int. J. Mod. Phys.* **C9**, 1439 (1998).
27. O. Filippova and D. Hänel, *J. Computat. Phys.* **158**, 139 (2000).
28. M. De Cicco, S. Succi, and G. Bella, *SIAM J. Scient. Comput.* **21**, 366 (1999).

29. K. Xu, *Gas-kinetic Schemes for Unsteady Compressible Flow Simulations*, VKI Lecture Series 1998-03 (VKI, Brussels, 1998); *J. Computat. Phys.* **171**, 289 (2001).
30. P. Lallemand and L.-S. Luo, submitted to *Phys. Rev.* **E** (2002).
31. A. Mezrhab, M. Bouzidi and P. Lallemand, submitted to *Comput. Fluids* (2002).
32. P. Lallemand and L.-S. Luo, *Phys. Rev.* **E61**, 6546 (2000).
33. D. d'Humières, M. Bouzidi, and P. Lallemand, *Phys. Rev.* **E63**, 066702 (2001).
34. D. d'Humières *et al.*, *Phil. Trans. R. Soc. Lond.* **A360**, 437 (2002).
35. L.-S. Luo *et al.*, *Phys. Rev.* **A43**, R7097 (1991).
36. E. Tric, G. Labrosse and M. Betrouni, *Int. J. Heat Mass Transfer* **43**, 4043 (2000).
37. F. Zhong, R. Ecke, and V. Steinberg, *Phys. Rev. Lett.* **67**, 2473 (1991).